

DOPING OF AlGaN ALLOYS

Chris G. Van de Walle,^{*} C. Stampfl,^{**} J. Neugebauer,^{**} M. D. McCluskey,^{*,a} N. M. Johnson^{*}

^{*}Xerox Palo Alto Research Center, 3333 Coyote Hill Road, Palo Alto, CA 94304

^{**}Fritz-Haber-Institut der Max-Planck-Gesellschaft, Faradayweg 4-6, D-14 195 Berlin-Dahlem, Germany

Cite this article as: MRS Internet J. Nitride Semicond. Res. 4S1, G10.4 (1999)

ABSTRACT

Nitride-based device structures for electronic and optoelectronic applications usually incorporate layers of $\text{Al}_x\text{Ga}_{1-x}\text{N}$, and n - and p -type doping of these alloys is typically required. Experimental results indicate that doping efficiencies in $\text{Al}_x\text{Ga}_{1-x}\text{N}$ are lower than in GaN. We address the cause of these doping difficulties, based on results from first-principles density-functional-pseudopotential calculations. For n -type doping we will discuss doping with oxygen, the most common unintentional donor, and with silicon. For oxygen, a DX transition occurs which converts the shallow donor into a negatively charged deep level. We present experimental evidence that oxygen is a DX center in $\text{Al}_x\text{Ga}_{1-x}\text{N}$ for $x > \sim 0.3$. For p -type doping, we find that compensation by nitrogen vacancies becomes increasingly important as the Al content is increased. We also find that the ionization energy of the Mg acceptor increases with alloy composition x . To address the limitations on p -type doping we have performed a comprehensive investigation of alternative acceptor impurities; none of the candidates exhibits characteristics that surpass those of Mg in all respects.

INTRODUCTION

Significant theoretical and experimental attention has been devoted to doping of GaN: which dopants to use, how to increase doping efficiency, what sources of compensation may occur, etc. For practical electronic and optoelectronic devices, however, it is essential to be able to control not just doping of GaN, but also of AlGaN alloys. For instance, AlGaN alloys form the thick cladding layers in nitride-based injection lasers, and the resistivity of these layers plays a major role in the device characteristics. Most research to date has indicated that AlGaN alloys are more difficult to dope than pure GaN, and the ability to dope AlGaN alloys significantly decreases with increasing Al content.

Several experimental studies have indicated a decrease in n -type conductivity of $\text{Al}_x\text{Ga}_{1-x}\text{N}$ with increasing x . Koide *et al.*¹ reported a decline in free electron concentration for $x > 0.2$. For unintentionally n -type doped AlGaN, Lee *et al.*² reported a rapid decrease in conductivity for $x > 0.4$. McCluskey *et al.*³ found a significant decrease in conductivity for $x > 0.3$ in unintentionally doped AlGaN samples; they were able to attribute the unintentional conductivity to oxygen. McCluskey *et al.* also found that intentional doping with silicon produced highly conductive material for $x = 0.44$. Bremser *et al.*^{4,5} also achieved intentional n -type doping with silicon up to $x = 0.42$, but for $x > 0.42$ addition of Si resulted in highly resistive films.

^a Present address: Department of Physics, Washington State University, P.O. Box 642814, Pullman, WA 99164-2814

The decrease in doping efficiency with increasing Al content is even more dramatic for *p*-type AlGa_xN. While *p*-type doping of pure GaN was originally a problem, those difficulties have largely been overcome due to the use of the Mg acceptor and the understanding of the role of hydrogen.^{6,7} For Al_xGa_{1-x}N, however, Bremser *et al.*^{4,5} reported a failure to achieve *p*-type conductivity with Mg doping for *x*>0.13. Other studies have also found a decrease in achievable hole concentration when the Al content of the AlGa_xN alloy is increased.^{8,9,10}

Useful information about the doping characteristics of nitride semiconductors can be obtained by performing first-principles calculations. We previously performed comprehensive studies of doping in *n*-type^{11,12} and *p*-type^{6,7,13} GaN. In order to address doping of AlGa_xN, we have first performed comprehensive studies of native defects and dopant and impurities in AlN.¹⁴ Many useful results for AlGa_xN alloys can be obtained by “interpolating” between the binary compounds.

First-principles calculations for native defects in AlN^{14,15,16} have yielded conclusions similar to those for GaN: self-interstitials and antisites are high in energy—with the exception of the Al interstitial in *cubic* AlN, which is a triple donor and could act as a compensating center in *p*-type material. The nitrogen vacancy is a high-energy defect in *n*-type AlN, but has a relatively low energy in *p*-type AlN. The behavior of V_{Al} is similar to V_{Ga} in GaN, but because of the larger band gap of AlN the formation energy of V_{Al} becomes significantly lower than V_{Ga} for Fermi-level positions high in the gap. The consequences of the behavior of these defects for doping will be explored in subsequent sections.

Our results identify two mechanisms that can reduce the *n*-type doping efficiency: (i) in the case of doping with oxygen (the most common unintentional donor), a *DX* transition occurs which converts the shallow donor into a negatively charged deep level^{3,17}; and (ii) cation vacancies (V_{Ga} or V_{Al}) act as triple acceptors and increase in concentration with alloy composition *x*. For *p*-type doping, we find that (i) nitrogen vacancies act as compensating centers and are more easily formed in AlN than in GaN; and (ii) the ionization energy of the Mg acceptor increases with alloy composition *x*.

The large ionization energy of Mg (around 200 meV) poses severe limitations on the ability to dope GaN, and this problem increases with increasing Al content in AlGa_xN alloys. It would be highly desirable to identify other *p*-type dopants that do not suffer from the limitations imposed by Mg. We have performed extensive investigations for a wide range of candidate acceptor species, addressing criteria such as solubility, ionization energy, and potential compensation due to interstitial configurations of the acceptor impurity; the results of this investigation will be discussed in the section on *p*-type doping.

METHODOLOGY

Our first-principles calculations are based on density-functional theory within the local density approximation (LDA) and using the pseudopotential-plane-wave method.^{18,19} We employ a supercell approach and use a tight-binding initialization scheme for the electronic wave functions.²⁰ Supercells containing 32 atoms were used to study the zinc-blende phase, and up to 96 atoms for the wurtzite phase. An energy cutoff of 40 Ry was used for AlN, with two or three special **k** points in the irreducible part of the Brillouin zone. The pseudopotentials were created using the scheme of Troullier and Martins.²¹

The formation energy of a defect in charge state *q* is expressed as

$$E^f(q) = E_{\text{defect}}^{\text{tot}}(q) - \sum_X n_X \mathbf{m}_X + qE_F \quad (1)$$

where $E_{\text{defect}}^{\text{tot}}(q)$ is the total energy of the defect and n_X and \mathbf{m}_X are the number and chemical potential of atoms of species *X*, respectively. E_F is the Fermi energy which is set to zero at the va-

lence-band maximum. In evaluating the chemical potentials, which depend on the experimental growth conditions, we assume thermal equilibrium: $\mathbf{m}_{\text{Ga}} + \mathbf{m}_{\text{N}} = \mathbf{m}_{\text{GaN}}$ for GaN, and $\mathbf{m}_{\text{Al}} + \mathbf{m}_{\text{N}} = \mathbf{m}_{\text{AlN}}$ for AlN. For convenience, we will display results for metal-rich conditions: \mathbf{m}_{Ga} is put equal to the energy of bulk Ga, or \mathbf{m}_{Al} is put equal to the energy of bulk Al. N-rich conditions would correspond to the chemical potential \mathbf{m}_{N} being determined by the energy of an N_2 molecule. The chemical potentials for the impurity species (O, Si, and Mg) are fixed by invoking equilibrium with Ga_2O_3 , Si_3N_4 , and Mg_3N_2 . For Li, Na, K, Be, Zn, and Ca, the chemical potentials of Li_3N , Na, K, Be_3N_2 , Zn_3N_2 , and Ca_3N_2 were used. Formation energies for general values of the chemical potential can always be obtained by referring back to Eq. (1).

RESULTS FOR N-TYPE DOPING

Our first-principles studies¹¹ as well as those of others^{15,22} have shown that the formation energy of the nitrogen vacancy in *n*-type GaN is too large for this defect to occur in any appreciable concentrations. We obtain similar results for the nitrogen vacancy in AlN. Figure 1 displays formation energies for native defects and donor impurities relevant for *n*-type AlN. For each defect we only show the line segment corresponding to the charge state that gives rise to the lowest energy at a particular value of E_F . The change in slope of the lines therefore represents a change in the charge state of the defect [see Eq. (1)]. Figure 1 applies to the zinc-blende phase and shows E_F spanning the theoretical (*GW*) band gap for zinc-blende AlN,²³ which is larger than the LDA band gap in our calculations (3.15 eV). Results for the wurtzite phase are very similar.

Figure 1 clearly shows that the formation energy of the nitrogen vacancy is significantly higher than that of oxygen and silicon, which behave as shallow donors. This indicates that the nitrogen vacancy is not the dominant center responsible for the *n*-type conductivity of $\text{Al}_x\text{Ga}_{1-x}\text{N}$.

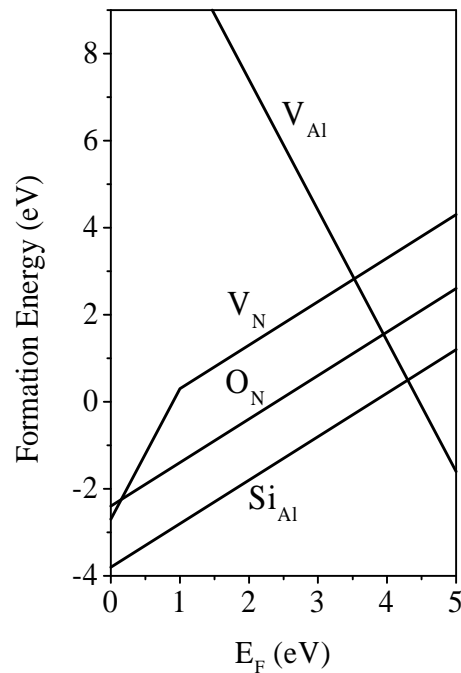


Figure 1: Formation energies as a function of Fermi level for defects and impurities relevant for *n*-type AlN, obtained from first-principles calculations for the zinc-blende phase, and assuming Al-rich conditions.

Unintentional doping – oxygen

Nitrogen vacancies were traditionally thought to be responsible for the large background *n*-type conductivity in GaN. In 1994 we proposed that not the nitrogen vacancy but oxygen and silicon impurities are responsible for unintentional *n*-type conductivity in GaN.¹² Oxygen had been proposed as a potential source of *n*-type conductivity in GaN as early as 1983.²⁴ Still, the prevailing conventional wisdom, attributing the *n*-type behavior to nitrogen vacancies, proved hard to overcome. Recent experiments have confirmed that unintentionally doped *n*-type GaN samples contain silicon or oxygen concentrations high enough to explain the electron concentrations. Götz *et al.*^{25,26} reported electrical characterization of intentionally Si-doped as well as unintentionally doped samples, and concluded that the *n*-type conductivity in the latter was due to silicon. They also found evidence of another shallow donor with a slightly higher activation energy, which was attributed to oxygen. Secondary-ion mass spectroscopy (SIMS) on hydride vapor phase epitaxy (HVPE) material also shows levels of oxygen or silicon in agreement with the electron concentration determined by electrical measurements.²⁶

Contaminating impurities may have many sources: water is the main contaminant of NH₃, the most frequently used source in metal-organic chemical deposition (MOCVD). The fact that even high-purity (99.999%) NH₃ can be a significant source of oxygen contamination was documented in the case of InGaN growth by Piner *et al.*²⁷ Fortunately, purification can remove most of the water. In MBE, oxygen may enter as a contaminant in the nitrogen source gas; or it may be due to the quartz lining of certain components, for instance plasma sources. We note that Götz *et al.*^{26,28} and Look and Molnar²⁹ have pointed out potential pitfalls in extracting information about dopant concentrations and ionization energies from Hall-effect measurements. Experiments on unintentionally doped HVPE-grown layers indicated the presence of a thin, highly conductive layer near the interface with the sapphire substrate. This layer acts as a parasitic, parallel conduction path. Götz *et al.*²⁶ suggested oxygen contamination may be responsible for the high conductivity of this layer.

The activation energy of oxygen has been determined from variable-temperature Hall effect measurements³⁰ to be 29 meV for a donor concentration $N_D=1\times 10^{18}$ cm⁻³. This activation energy decreases with increasing donor concentration. Götz *et al.* also reported that the total oxygen concentration (measured by SIMS) was significantly higher than the donor concentration. We suggest that such additional oxygen may occur in the form of Ga₂O₃ precipitates.

Hydrostatic pressure offers a very useful tool to explore the cause and behavior of *n*-type conductivity in GaN.^{31,32} Freeze-out of carriers was reported under application of hydrostatic pressure greater than 20 GPa. These findings can be explained by the behavior of oxygen, which undergoes a transition from a shallow to a deep *DX* center in wurtzite GaN under pressure.^{17,32,33} The stable shallow center at the *equilibrium* volume of GaN corresponds to oxygen at the substitutional nitrogen site. The *DX* geometry corresponds to an oxygen atom moving off the substitutional position along the [0001] direction. This geometry becomes stable under hydrostatic pressure. The associated induced electronic state is a highly localized deep level. In the *DX* configuration the defect is negatively charged, i.e., it is a deep acceptor, and will therefore trap free carriers. The stability of the localized deep *DX* state is attributed to interactions between the negatively charged oxygen impurity and a third-nearest-neighbor cation along the *c* axis: we have proposed that a Coulombic attraction is the driving force for the large lattice relaxation that stabilizes the *DX* geometry.¹⁷ In the zinc-blende structure, these third-nearest-neighbor atoms occur in different positions in the lattice; the formation of the *DX* configuration is correspondingly suppressed in the zinc-blende phase.

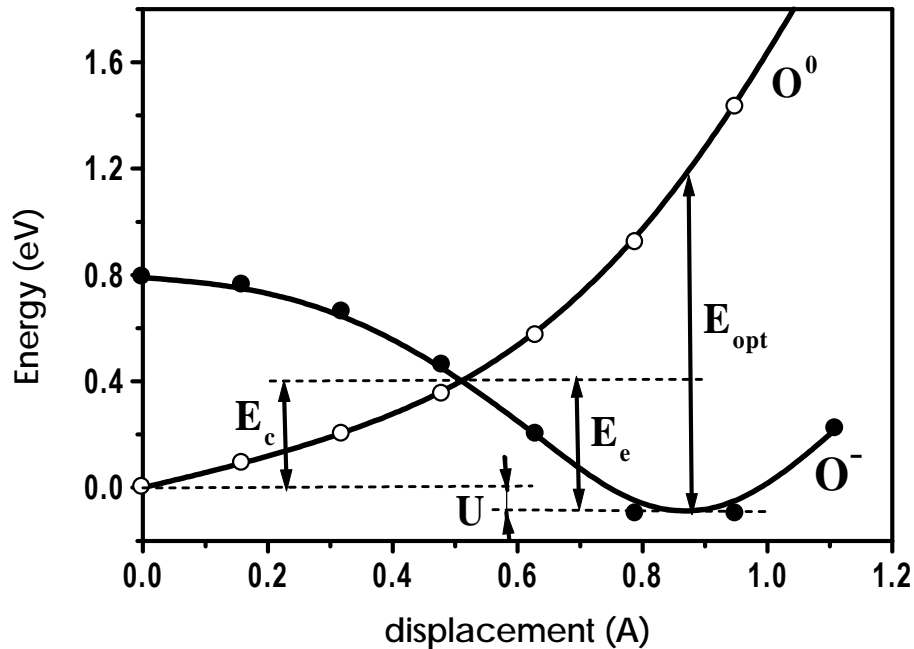


Figure 2: Configuration coordinate diagram for oxygen displacements along [0001] in AlGaN, based on first-principles calculations for GaN:O and AlN:O. E_{opt} is the optical ionization energy; E_c and E_e are the capture and emission barriers.

Alloying with AlN increases the band gap of GaN in a similar way to hydrostatic pressure. *DX* center formation is therefore also expected to occur in $\text{Al}_x\text{Ga}_{1-x}\text{N}$. Indeed, our computational studies showed that the *DX* configuration is the stable state for the oxygen impurity in wurtzite (but not zinc-blende) AlN.¹⁷ Figure 2 shows a configuration coordinate diagram for oxygen displacements in AlGaN. The data points were obtained from first-principles calculations for oxygen in GaN and in AlN, based on an interpolation for the case where the *DX* configuration is 0.1 eV lower in energy than the substitutional donor.

The configuration coordinate diagram is characteristic of a metastable center: for zero displacement, the impurity is located on the substitutional site and behaves as a shallow donor. However, a second minimum occurs in the diagram, corresponding to a large displacement of the impurity (close to 1 Å) and a different (negative) charge state. For $x < 0.3$, this second minimum is higher in energy than the on-site, shallow-donor configuration. However, for $x > 0.3$, the second minimum becomes lower in energy, as illustrated in Fig. 2. The *DX* state is then the lowest-energy state of the system; however, electrons can be emitted out of the *DX* state, and since there is a barrier (E_c) to capturing them again, one expects to observe persistent photoconductivity, at least at low temperatures. The mechanism to release electrons out of the *DX* state can be either thermal (with an activation energy E_e) or optical, with a threshold E_{opt} .

Experimental confirmation for this model has come from Hall effect and persistent photoconductivity measurements on unintentionally doped AlGaN samples with Al content up to $x=0.39$.³ The samples were MOCVD grown, with a thickness of 1 μm, and Al concentrations were determined by x-ray diffraction, assuming relaxed layers and Vegard's law. Concentrations of Si and oxygen impurities were measured by SIMS. Unintentionally doped AlGaN showed

oxygen concentrations of approximately 10^{19} cm^{-3} and silicon concentrations of 10^{18} cm^{-3} , indicating that the conductivity of the samples was due to oxygen. Variable-temperature Hall effect measurements showed a freezeout of the free electrons with decreasing temperature, characterized by an activation energy that increased with Al concentration in the alloy. The activation energy E_{DX} was determined by exponential fits to the Hall effect data. The decrease in the free electron concentration can be explained by an increase in E_{DX} . This increase in the donor binding energy is consistent with a deep DX level which becomes stable (has a lower energy than the conduction-band minimum) for $x > 0.27$, in good agreement with the theoretical prediction. This result is also consistent with the experiments on GaN:O under pressure: the band gap of GaN at 20 GPa is approximately 0.8 eV higher than at ambient pressure, and a similar increase in band gap is found when alloying with AlN with x between 0.3 and 0.4.

Persistent photoconductivity is a direct manifestation of metastability, characteristic of centers with a large difference in lattice relaxation between two metastable states. Persistent photoconductivity was observed in $\text{Al}_x\text{Ga}_{1-x}\text{N}$ epilayers with $x \geq 0.39$ at temperatures below 150 K. The persistent photoconductivity decreases with time, because oxygen centers return from the shallow to the deep state. In doing so, they need to surmount the barrier (Fig. 2). The temperature range in which this transition was observed was between 120 and 150 K; this is consistent with the barrier E_c of about 0.4 eV emerging from our calculations.

To measure the optical cross section of absorption for the DX centers, the photocurrent was measured for photon energies from 1.0 to 1.5 eV. An optical threshold of about 1.3 eV was found, again in good agreement with the theoretical prediction shown in Fig. 2.

While the observation of persistent photoconductivity is one of the distinguishing features of metastable DX centers, it should be pointed out that observations of persistent photoconductivity are not *necessarily* indicative of the presence of DX -like centers. Various groups have reported persistent photoconductivity in n -type GaN.^{34,35} Those observations show photoconductivity at room temperature, while our observations for DX centers only show photoconductivity for temperature below 150 K. In addition, the optical absorption threshold was found to be greater than 2 eV, again inconsistent with the observations for DX centers. The behavior observed in Refs. 34 and 35 may be due to other types of point defects, or to the presence of defective regions near extended defects.

For oxygen, we must conclude that it cannot be used as a shallow donor in $\text{Al}_x\text{Ga}_{1-x}\text{N}$ with $x > 0.3$. Even if another donor impurity is used (such as silicon, see below) that does not exhibit DX behavior, the presence of oxygen in the layer could be detrimental to n -type conductivity: indeed, once oxygen undergoes the DX transition it behaves as an acceptor, and therefore counteracts the electrical activity of other donors. Control of oxygen incorporation in $\text{Al}_x\text{Ga}_{1-x}\text{N}$ with high Al content is therefore essential.

Doping with Silicon

Silicon is almost universally used for intentional n -type doping of GaN, AlGa_N, and InGa_N. Silicon doping is typically achieved by flowing SiH_4 during MOCVD growth, or using a solid Si source in MBE. The formation energies shown in Fig. 1 show that the formation energy of silicon is quite low in AlN, and therefore it is readily incorporated in AlN as well as in GaN. The activation energy of silicon in GaN derived from variable-temperature Hall effect measurements^{25,30} is 17 meV for $N_D = 3 \times 10^{17} \text{ cm}^{-3}$. As pointed out in the case of oxygen, the ionization energy is sensitive to the concentration of the dopant.

Our calculations for silicon in GaN under pressure, and in AlN, indicate that silicon donors do not exhibit the DX transition.¹⁷ The difference with oxygen can be understood on the basis of the different location in the lattice. While oxygen substitutes on a *nitrogen* site, silicon sits on a

substitutional *cation* site. In that position, the third nearest neighbor is a *nitrogen* atom. In the *DX* state, the silicon would become negatively charged, and would thus experience a Coulomb repulsion from the third-nearest-neighbor anion; this repulsion suppresses the *DX* formation. Silicon was indeed experimentally found to remain a shallow donor in GaN under pressure up to 25 GPa.³² For $\text{Al}_x\text{Ga}_{1-x}\text{N}$ alloys with $x=0.44$ we found that intentional doping with silicon resulted in a free-electron concentration close to the silicon concentration ($8 \times 10^{18} \text{ cm}^{-3}$, as measured by SIMS). It was also found, however, that even in the intentionally Si-doped sample a background of oxygen was present (at a level of $3 \times 10^{18} \text{ cm}^{-3}$). Those oxygen atoms can still undergo the *DX* transition, effectively becoming compensating centers. It is important, therefore, to suppress oxygen incorporation when growing Si-doped $\text{Al}_x\text{Ga}_{1-x}\text{N}$ with high x .

The negative impact of unintentional oxygen incorporation on the conductivity of Si-doped AlGaN is a likely explanation for the experimental observations of Polyakov *et al.*^{36,37} They found that the free electron concentration decreases with increasing Al content of the alloy. The increase in Al content also led to an increase in the density of defects with energy levels deeper than silicon, leading to increased difficulty in *n*-type doping of the alloy. Polyakov *et al.* also reported persistent photoconductivity in their samples. The observations of Polyakov *et al.* can be consistently explained by assuming that oxygen is unintentionally incorporated, a possibility that was recognized by Polyakov *et al.* The decrease in electron concentration for $x \geq 0.3$ is then due to the formation of oxygen *DX* centers; in the negatively charged *DX* state, oxygen effectively acts as an acceptor, compensating the *n*-type conductivity introduced by the Si donors. The characteristics of the persistent photoconductivity (capture and emission barrier, and optical ionization energy) are consistent with those obtained for oxygen *DX* centers³ and in our first-principles calculations (see Fig. 2).

Unintentional incorporation of oxygen may also explain the decrease in *n*-type conductivity in Si-doped $\text{Al}_x\text{Ga}_{1-x}\text{N}$ for $x > 0.42$ observed by Bremser *et al.*^{4,5} We should point out, however, that even in the absence of oxygen a compensation mechanism may occur, namely due to cation vacancies. In GaN, compensation of Se donors by Ga vacancies was observed by Yi and Wessels.³⁸ The calculated defect formation energy for the Al vacancy is shown in Fig. 1, for Al-rich conditions in AlN. For *n*-type conditions (E_F high in the gap), silicon donors will suffer from some degree of compensation by triply ionized Al vacancies. The behavior of V_{Al} is similar to V_{Ga} in GaN,¹¹ but because of the larger band gap of AlN the formation energy of V_{Al} in AlN becomes significantly lower than that of V_{Ga} in GaN for Fermi-level positions high in the gap. Cation vacancies thus become an increasingly important source of donor compensation as the Al content x is increased in $\text{Al}_x\text{Ga}_x\text{N}$.

RESULTS FOR *P*-TYPE DOPING

Magnesium has emerged as the *p*-type dopant of choice for GaN. Still, the hole concentration that can be achieved is lower than desired, particularly for applications such as high *p*-type doping near metal contacts for improved Ohmic contact behavior. In addition, the hole concentration that can be achieved with Mg doping has been observed to decrease rapidly with increasing Al content x in $\text{Al}_x\text{Ga}_{1-x}\text{N}$.^{5,8,9,10} Magnesium exhibits no tendency to form deep levels (so called *AX* levels, analogous to *DX* for donors),³³ thus ruling out a shallow-deep transition as the source of the drop in hole concentration. We also found, for Mg in GaN, that incorporation of Mg on interstitial sites, or on nitrogen sites, is energetically unfavorable.³⁹ The main issue limiting the hole concentration achievable with Mg in GaN is the solubility.

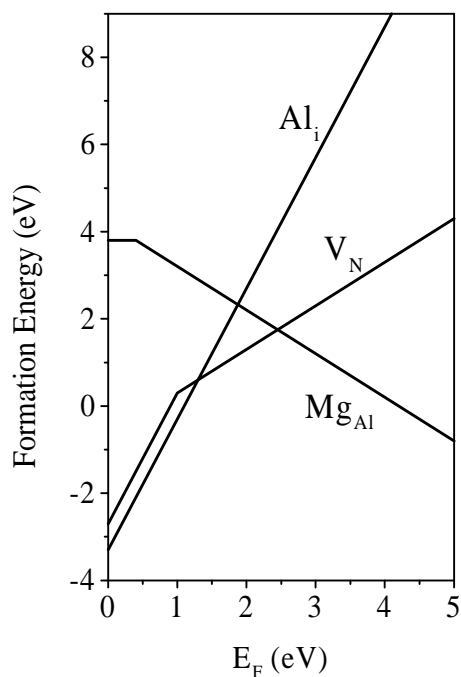
Our calculations for the Mg acceptor in AlN indicate that its ionization energy (0.4 eV) is higher than in GaN (0.2 eV), as can be seen from Fig. 3 (the ionization energy corresponds to the Fermi level positions where the formation energies of Mg^0 and Mg^- are equal). This increase in

the ionization energy leads to a decrease in doping efficiency. Based on an analysis of temperature-dependent Hall data Tanaka *et al.* found the Mg activation energy to be 35 meV deeper in $\text{Al}_{0.08}\text{Ga}_{0.92}\text{N}$ than in GaN.⁸ Assuming linearity, this would make the Mg acceptor in AlN 0.44 eV deeper than in GaN.

Compensation by native defects is another important mechanism that may contribute to the decline in hole concentrations. Fig. 3 shows that two defects with low formation energies may inhibit successful *p*-type doping of $\text{Al}_x\text{Ga}_{1-x}\text{N}$, namely the nitrogen vacancy and the cation interstitial. The cation interstitial has a low formation energy in zinc-blende material, but is much higher in energy in wurtzite. The nitrogen vacancy has a strikingly lower formation energy in AlN than in GaN, and it may play an important role in *p*-type GaN and AlGaN. The formation energy of the nitrogen vacancy is too high for it to be incorporated in *n*-type GaN, but as can be seen from Fig. 3, this formation energy becomes significantly lower in *p*-type material. During MOCVD growth the formation of nitrogen vacancies is suppressed because hydrogen also behaves as a compensating donor, and has a lower formation energy.⁷ Still, a certain concentration of nitrogen vacancies will be incorporated, and we propose that these vacancies are at least partially responsible for the decreased doping efficiency of Mg when the Al content is raised in $\text{Al}_x\text{Ga}_{1-x}\text{N}$ alloys.

For certain values of the Fermi level, some formation energies in Figs. 1 and 3 become negative; one may wonder about the physical meaning of negative formation energies. Inspection of the plots, however, will make clear that physically meaningful positions of the Fermi level will always produce positive formation energies. Indeed, the Fermi energy is determined by the condition of charge neutrality; for Fermi-level positions far from the band edges, this requires having equal numbers of positively and negatively charged defects or impurities (if they are singly charged). The Fermi level will therefore be pinned near the point where the formation energies of the dominant donor and acceptor are equal. The plots then show that this value of the Fermi level corresponds to positive formation energies.

Figure 3: Formation energies as a function of Fermi level for defects and impurities relevant for *p*-type AlN, obtained from first-principles calculations for the zinc-blende phase, and assuming Al-rich conditions. We note that the formation energy of Al_i is significantly higher in *wurtzite* AlN.



The nitrogen vacancy (V_N) behaves as a donor which can donate one, two, or three electrons. Only the V_N^+ and V_N^{3+} charge states are found to be stable; the V_N^{2+} state is unstable, presenting a so-called negative- U effect. This behavior is similar to that calculated for nitrogen vacancies in GaN.⁴⁰ However, the +/3+ transition level occurs at a higher position in the band gap in the case of AlN (around 1 eV). Because the formation energy decreases much faster with decreasing Fermi level in the 3+ charge state, the nitrogen vacancy becomes much more favorable for low Fermi-level positions in AlN.

The +/3+ transition is characterized by a large lattice relaxation.⁴⁰ Defects with large lattice relaxations are often responsible for persistent photoconductivity (as we saw in the case of oxygen DX centers). The presence of nitrogen vacancies may therefore be responsible for the observed persistent photoconductivity effects in p -type GaN.^{41,42,43} The nitrogen vacancy may also give rise to the blue lines (around 2.9 eV) commonly observed by photoluminescence in Mg-doped GaN.^{33,43,44,45,46} The appearance and disappearance of photoluminescence (PL) lines during post-growth annealing of Mg-doped layers grown by MOCVD^{47,48} may be related to the interactions of hydrogen with nitrogen vacancies. Complexes between hydrogen and nitrogen vacancies can form during growth⁴³; the calculated binding energy of the V_NH^{2+} complex, expressed with respect to interstitial H in the positive charge state, is 1.56 eV. Dissociation of this complex, producing isolated nitrogen vacancies, may explain the behavior of PL lines during annealing for acceptor activation.⁴³

Alternative Acceptors

Despite the successes achieved with Mg, p -type doping levels in GaN and AlGaN alloys are lower than desirable for low-resistance cladding layers and Ohmic contacts. Achieving higher hole concentrations with Mg as the dopant has proved difficult. It would therefore be desirable to identify acceptors that are superior to Mg.

The performance of an acceptor can be judged on the basis of three main criteria: (i) solubility; (ii) stability against compensation by other configurations of the acceptor dopant (e.g., interstitials); and (iii) depth of the acceptor level (ionization energy). Each of these aspects can be addressed on the basis of results obtained from first-principles calculations. The *solubility* of a substitutional acceptor corresponds to the equilibrium concentration of the impurity in the lattice, which is determined by the formation energy. The formation energy of the impurity in configurations other than the substitutional site determines the likelihood of incorporation on those sites. Interstitial configurations tend to be favorable for elements with a small atomic radius, such as Li or Be.

Previous theoretical investigations^{13,49,50} have not produced any candidate with characteristics exceeding those of Mg in all respects. Our own results show that the column-II acceptors perform noticeably better than those from column I; the latter suffer from poor solubility. Lithium also suffers from incorporation on interstitial sites, where it acts as a donor. Among column-II acceptors, Ca and heavier elements also have high formation energies and hence poor solubility. The calculated ionization energies for Zn and Ca are larger than for Mg. The smallest column-II element, Be, has a solubility comparable to Mg. Its calculated ionization energy is slightly smaller than Mg, but the difference is within the error bar of the computation and hence not conclusive.⁵⁰ Because it is a small atom, Be may suffer from incorporation on interstitial sites, where it acts as a donor, thus causing self-compensation.

Experimental work on acceptors other than Mg has been very limited. Bergman *et al.* used photoluminescence (PL) to derive an ionization energy of 0.34 eV for Zn.⁵¹ Doping with Zn has not resulted in p -type conductivity, presumably due to the large ionization energy of the Zn acceptor. Experimental results about Be are inconclusive: Brandt *et al.* have reported high levels

of *p*-type doping using Be in MBE, provided oxygen is present as a co-dopant.^{52,53} This result is difficult to understand based on equilibrium thermodynamics, as pointed out by Bernardini *et al.*⁵⁰ Other work has indicated Be indeed acts as an acceptor; results about the ionization energy are based on luminescence, with Salvador *et al.* finding a relatively large ionization energy (250 meV),⁵⁴ Ronning *et al.* finding 150 meV,⁵⁵ and Sánchez *et al.* deriving a much smaller value (90 meV).⁵⁶

To our knowledge, experimental studies of other acceptor impurities have only been performed using ion implantation (see, e.g., Ref. 57). Unfortunately, implantation damage is very difficult to remove by annealing in GaN, due to the hardness of the lattice and the low diffusivity. The presence of implantation defects then makes it difficult to reliably assess the properties of the implanted acceptors, and in our opinion no conclusive results have been obtained.

CONCLUSIONS

We have reported a comprehensive investigation of impurities and defects in AlN and GaN, from which we have drawn conclusions about the limitations on doping in $\text{Al}_x\text{Ga}_{1-x}\text{N}$ alloys. Our first principles calculations indicate that the *DX* behavior of oxygen and compensation by the cation vacancy are responsible for the decrease in *n*-type conductivity in $\text{Al}_x\text{Ga}_{1-x}\text{N}$ with increasing *x*. With respect to *p*-type doping of $\text{Al}_x\text{Ga}_{1-x}\text{N}$, our results show that the nitrogen vacancy becomes an increasingly dominant compensating center as *x* increases. We also observe an increase in the Mg ionization energy with increasing Al content. Investigations of a wide range of potential alternative acceptors show that none emerge as being superior to Mg; Be may be a possibility, but could suffer from compensation by Be interstitials.

ACKNOWLEDGMENTS

We acknowledge fruitful collaborations with D. P. Bour, M. Kneissl, W. Walukiewicz, and W. Götz. This work was supported in part by DARPA under agreement no. MDA972-96-3-0014. C. Stampfl and J. Neugebauer gratefully acknowledge support from the DFG (Deutsche Forschungsgemeinschaft).

REFERENCES

- ¹ Y. Koide, H. Itoh, N. Sawaki, I. Akasaki, and M. Hashimoto, *J. Electrochem. Soc.*, **133**, 1956 (1986).
- ² H. G. Lee, M. Gershenson, B. L. Goldenberg, *J. Elec. Mat.* **20**, 621 (1991).
- ³ M. D. McCluskey, N. M. Johnson, C. G. Van de Walle, D. P. Bour, M. Kneissl, and W. Walukiewicz, *Phys. Rev. Lett.* **80**, 4008 (1998).
- ⁴ M. D. Bremser, W. G. Perry, T. Zheleva, N. V. Edwards, O. H. Nam, N. Parikh, D. E. Aspnes, and R. F. Davis, *MRS Internet J. Nitride Semicond. Res.* **1**, 8 (1996).
- ⁵ M. D. Bremser, W. G. Perry, N. V. Edwards, T. Zheleva, N. Parikh, D. E. Aspnes, and R. F. Davis, *Mat. Res. Soc. Symp. Proc.* **395**, 195 (1996).
- ⁶ J. Neugebauer and C. G. Van de Walle, *Phys. Rev. Lett.* **75**, 4452 (1995).
- ⁷ J. Neugebauer and C. G. Van de Walle, *Appl. Phys. Lett.* **68**, 1829 (1996).
- ⁸ T. Tanaka, A. Watanabe, H. Amano, Y. Kobayashi, I. Akasaki, S. Yamazaki, and M. Koike, *Appl. Phys. Lett.* **65**, 593 (1994).

- ⁹ M. Katsuragawa, S. Sota, M. Komori, C. Anbe, T. Takeuchi, H. Sakai, H. Amano, and I. Aka-saki, *J. Cryst. Growth* **189/190**, 528 (1998).
- ¹⁰ M. Suzuki, J. Nishio, M. Onomura, and C. Hongo, *J. Cryst. Growth* **189/190**, 511 (1998).
- ¹¹ J. Neugebauer and C. G. Van de Walle, *Phys. Rev. B* **50**, 8067 (1994).
- ¹² J. Neugebauer and C. G. Van de Walle, in *Proceedings of the 22nd International Conference on the Physics of Semiconductors* (World Scientific, Singapore, 1995), p. 2327.
- ¹³ J. Neugebauer and C. G. Van de Walle, in *Proceedings of the 23rd International Conference on the Physics of Semiconductors* (World Scientific, Singapore, 1996) p. 2849.
- ¹⁴ C. Stampfl and C. G. Van de Walle, *Appl. Phys. Lett.* **72**, 459 (1998).
- ¹⁵ T. Mattila and R. M. Nieminen, *Phys. Rev. B* **54**, 16676 (1996).
- ¹⁶ T. Mattila and R. M. Nieminen, *Phys. Rev. B* **55**, 9571 (1997).
- ¹⁷ C. G. Van de Walle, *Phys. Rev. B* **57**, R2033 (1998).
- ¹⁸ R. Stumpf and M. Scheffler, *Computer Phys. Commun.* **79**, 447 (1994)
- ¹⁹ M. Bockstedte, A. Kley, J. Neugebauer, and M. Scheffler, *Comp. Phys. Commun.* **107**, 187 (1997).
- ²⁰ J. Neugebauer and C. G. Van de Walle, *Mater. Res. Soc. Symp. Proc.* **408**, 43 (1996).
- ²¹ N. Troullier and J. L. Martins, *Phys. Rev. B* **43**, 1993 (1991).
- ²² P. Boguslawski, E. L. Briggs, and J. Bernholc, *Phys. Rev. B* **51**, 17255 (1995).
- ²³ A. Rubio, J. L. Corkhill, M. L. Cohen, E. Shirley, and S. G. Louie, *Phys. Rev. B* **48**, 11810 (1993).
- ²⁴ W. Seifert, R. Franzheld, E. Butter, H. Sobotta, and V. Riede, *Cryst. Res. & Technol.* **18**, 383 (1983).
- ²⁵ W. Götz, N. M. Johnson, C. Chen, H. Liu, C. Kuo, and W. Imler, *Appl. Phys. Lett.* **68**, 3144 (1996).
- ²⁶ W. Götz, J. Walker, L. T. Romano, and N. M. Johnson, *Mat. Res. Soc. Symp. Proc.* **449**, 525 (1997).
- ²⁷ E. L. Piner, M. K. Behbehani, N. A., El-Masry, J. C. Roberts, F. G. McIntosh, and S. M. Be-dair, *Appl. Phys. Lett.* **71**, 2023 (1997).
- ²⁸ W. Götz, L. T. Romano, J. Walker, N. M. Johnson, and R. J. Molnar, *Appl. Phys. Lett.* **72**, 1214 (1998).
- ²⁹ D. C. Look, and R. J. Molnar, *Appl. Phys. Lett.* **70**, 3377 (1997).
- ³⁰ W. Götz, R. S. Kern, C. H. Chen, H. Liu, D. A. Steigerwald, and R. M. Fletcher, *Mater. Sci. and Engin. B* (in press).
- ³¹ P. Perlin, T. Suski, H. Teisseyre, M. Leszczynski, I. Grzegory, J. Jun, S. Porowski, P. Boguslawski, J. Bernholc, J. C. Chervin, A. Polian, and T. D. Moustakas, *Phys. Rev. Lett.* **75**, 296 (1995).
- ³² C. Wetzell, T. Suski, J. W. Ager III, E. R. Weber, E. E. Haller, S. Fischer, B. K. Meyer, R. J. Molnar, and P. Perlin, *Phys. Rev. Lett.* **78**, 3923 (1997).
- ³³ C. H. Park and D. J. Chadi, *Phys. Rev. B* **55**, 12 995 (1997).
- ³⁴ M. T. Hirsch, J. A. Wolk, W. Walukiewicz, and E. E. Haller, *Appl. Phys. Lett.* **71**, 1098 (1997).
- ³⁵ A. E. Wickenden, G. Beadie, D. D. Koleske, W. S. Rabinovich, and J. A. Freitas, Jr., *Mat. Res. Soc. Symp. Proc.* **449**, 531 (1997).
- ³⁶ A. Y. Polyakov, M. Shin, J. A. Freitas, M. Skowronski, D. W. Greve, and R. G. Wilson, *J. Appl. Phys.* **80**, 6349 (1996).
- ³⁷ A. Y. Polyakov, N. B. Smirnov, A. V. Govorkov, M. G. Mil'vidskii, J. M. Redwing, M. Shin, M. Skowronski, D. W. Greve, and R. G. Wilson, *Solid-State Electronics* **42**, 627 (1998).
- ³⁸ G.-C. Yi, and B. W. Wessels, *Appl. Phys. Lett.* **69**, 3028 (1996).

-
- ³⁹ J. Neugebauer and C. G. Van de Walle, Proc. Mater. Res. Soc. Symp. **395**, 645 (1996).
- ⁴⁰ J. Neugebauer and C. G. Van de Walle, in Festkörperprobleme/Advances in Solid State Physics, Vol. **35**, edited by R. Helbig (Vieweg, Braunschweig/Wiesbaden, 1996) p. 25.
- ⁴¹ J. Z. Li, J. Y. Lin, H. X. Jiang, A. Salvador, A. Botchkarev, and H. Morkoç, Appl. Phys. Lett. **69**, 1474 (1996).
- ⁴² C. Johnson, J. Y. Lin, H. X. Jiang, M. A. Khan, C. J. and Sun, Appl. Phys. Lett. **68**, 1808 (1996).
- ⁴³ C. G. Van de Walle, Phys. Rev. B **56**, R10 020 (1997).
- ⁴⁴ M. Leroux, B. Beaumont, N. Grandjean, P. Lorenzini, S. Haffouz, P. Vennéguès, J. Massies, and P. Gibart, Mat. Sci. Engin. B. **50**, 97 (1997).
- ⁴⁵ U. Kaufmann, M. Kunzer, M. Maier, H. Obloh, A. Ramakrishnan, B. Santic, and P. Schlotter, Appl. Phys. Lett. **72**, 1326 (1998).
- ⁴⁶ F. Calle, E. Monroy, F. J. Sánchez, E. Muñoz, B. Beaumont, S. Haffouz, M. Leroux, and P. Gibart, MRS Internet J. Nitride Semicond. Res. **3**, 24 (1998).
- ⁴⁷ S. Nakamura, N. Iwasa, M. Senoh, and T. Mukai, Jpn. J. Appl. Phys. **31**, 1258 (1992).
- ⁴⁸ W. Götz, N. M. Johnson, J. Walker, D. P. Bour, and R. A. Street, Appl. Phys. Lett. **68**, 667 (1996).
- ⁴⁹ V. Fiorentini, F. Bernardini, A. Bosin, and D. Vanderbilt, in *Proceedings of the 23rd International Conference on the Physics of Semiconductors*, edited by M. Scheffler, and R. Zimmermann (World Scientific, Singapore, 1996), p. 2877.
- ⁵⁰ F. Bernardini, V. Fiorentini, and A. Bosin, Appl. Phys. Lett. **70**, 2990 (1997).
- ⁵¹ P. Bergman, G. Ying, B. Monemar, and P. O. Holtz, J. Appl. Phys. **61**, 4589 (1987).
- ⁵² O. Brandt, H. Yang, H. Kostial, and K. H. Ploog, Appl. Phys. Lett. **69**, 2707 (1996).
- ⁵³ K. H. Ploog and O. Brandt, J. Vac. Sci. Technol. A. **16**, 1609 (1998).
- ⁵⁴ A. Salvador, W. Kim, Ö. Aktas, A. Botchkarev, Z. Fan, and H. Morkoç, Appl. Phys. Lett. **69**, 2692 (1996).
- ⁵⁵ C. Ronning, E. P. Carlson, D. B. Thomson, and R. F. Davis, Appl. Phys. Lett. **73**, 1622 (1998).
- ⁵⁶ F. J. Sánchez, F. Calle, M. A. Sánchez-García, E. Calleja, E., Muñoz, C. H. Molloy, D. J. Somerford, F. K. Koschnick, K. Michael, and J. M. Spaeth, MRS Internet J. Nitride Semicond. Res. **3**, 19 (1998).
- ⁵⁷ J. W. Lee, S. J. Pearton, J. C. Zolper, and R. A. Stall, Appl. Phys. Lett. **68**, 2102 (1996).